IEEE Access
Multidisciplinary | Rapid Review | Open Access Journal

Received March 23, 2020, accepted April 20, 2020, date of publication April 28, 2020, date of current version May 14, 2020.

Digital Object Identifier 10.1109/ACCESS.2020.2990927

A Particle Swarm Optimization Algorithm Based on Time-Space Weight for Helicopter Maritime Search and Rescue Decision-Making

ZIKUN CHEN[1], HU LIU[1], YONGLIANG TIAN[1], RUI WANG[1], PEISEN XIONG[1], AND GUANGHUI WU[1,2]

[1]School of Aeronautic Science and Engineering, Beihang University, Beijing 100083, China
[2]Commercial Aircraft Corporation of China Ltd., Shanghai 200210, China

Corresponding author: Yongliang Tian (tianyongliang_buaa@163.com)

This work was supported by the Research Project from Ministry of Industry and Information Technology of People's Republic of China.

ABSTRACT One of the important problems to be solved in maritime search and rescue (MSAR) is decision-making, and the premise of it is determining the mission area for search and rescue unit. To solve the problem that classical cellular iterative search (CIS) algorithm is easy to fall into local optimal solution when determining the mission area, the particle swarm optimization algorithm based on time-space weight (TS-PSO) is proposed in this paper. This algorithm summarizes the optimization objectives and constraint conditions of the MSAR mission area planning according to search theory, carries out the parametric modeling of mission area legitimately and obtains the global optimal solution by continuous exploration in the parameter definition domain. On this basis, by analyzing the time-space weight of drift prediction data, the optimization results are further improved. Finally, through the case simulation analysis, it can be seen that the TS-PSO algorithm can effectively make up for the deficiency of the CIS algorithm and further improve the success probability of optimal MSAR mission area.

INDEX TERMS Global optimal solution, maritime search and rescue, mission area planning, particle swarm optimization algorithm, time-space weight.

I. INTRODUCTION

In helicopter maritime search and rescue (MSAR) mission, it is of great significance for reducing the loss of life and property that distressed facilities, vessels and people are found and rescued efficiently, the decisive factor of which is the accurate positioning of optimal mission area. According to the search theory [1]–[3], it can be known that the probability of success (POS), which is calculated from the probability of coverage (POC) and the probability of detection (POD), can be used to judge the pros and cons of MSAR mission area. Then the POS value can be optimized to the highest by parameter adjustment. The determination of optimal mission area is conductive for search and rescue unit (SARU) to find search and rescue target (SART) efficiently, thereby achieving a higher mission success rate. Therefore, the mission area planning is a primary concern of decision-making issues.

The associate editor coordinating the review of this manuscript and approving it for publication was Rosario Pecora.

In recent years, many scholars have done massive researches on the MSAR mission area planning, and a lot of MSAR decision-making systems have been also widely used, such as SARMAP [4], SAROPS [5] and CASP [6], etc. The cellular iterative search (CIS) algorithm is a common algorithm in mission area planning, which can find the optimal mission area under current conditions by obtaining drift prediction data through integrating GIS and marine environment database. In addition, the improvement and optimization of CIS algorithm is one of the important research directions in this issue. For example, Xiao [7] established the optimal searching rectangle allocation algorithm, which used folding seeking method to allocate searching rectangles under constraints and optimizes POS value to the maximum. Agbissoh *et al.* [8], further used CIS algorithm to plan mission area, which obtained the rectangular region with the highest POS value by iteratively extending based on grid partition of given predicted discrete points and using the grid with the highest POC value as a benchmark.

At the same time, heuristic algorithms [9], [10] like particle swarm optimization algorithm (PSO) [11] are also widely applied in MSAR. Rafferty and McGookin [12], designed an autonomous air-sea search and rescue system, which planned the helicopter search path in a given region based on PSO algorithm, and obtained a better path than random search proved by simulation analysis. Lv *et al.* [13], proposed an improved PSO algorithm to solve the searching problem of discrete maritime static targets, where the sub-region importance evaluation function was established in order to maximize the POS value of plan within a certain time. Based on PSO algorithm, Liu *et al.* [14], developed the continuous-discrete PSO (CDPSO) algorithm to generate multi-agent shape formation, and illustrated the application of the algorithm in conjunction with the MH370 search and rescue process. Ye *et al.* [15], provided a simulation-based multi-agent PSO (SA-PSO) algorithm, which supported marine oil spill decision-making by integrated simulation and optimization of response device allocation and process control. Sánchez-García *et al.* [16], proposed a distributed and dynamic PSO algorithm for UAV networks (dPSO-U), which took the victims movements and the communication among UAVs into consideration, to generate trajectories for drone formations in large-scale disaster scenarios. Simulation results showed that this algorithm could find target faster. Wang *et al.* [17], proposed various path planning algorithms based on distributed particle swarm optimization (DPSO) for UAV swarms, which were MDC-DPSO, FCO-DPSO, ACE-PSO, and the simulation results showed that these algorithms could effectively meet the requirements of detection time and accuracy. These studies provide feasible methods for exploring the global optimal solution of mission area. However, there is no previous study about the application of PSO algorithm in helicopter MSAR mission area planning, which will be a useful way for decision-maker to solve this problem.

Through in-depth study, it can be seen that the classical CIS algorithm, which is the main algorithm in mission area planning, can obtain more optimal mission area. However, the insufficient analysis of SART drift prediction data and the inflexibility of grid partition when explore optimal mission area often leads to local optimal solutions. Therefore, aiming at these shortcomings of it, a particle swarm optimization algorithm based on space-time weight (TS-PSO) is proposed in this paper to solve this problem in helicopter MSAR mission area planning. According to the classical search theory, the optimization objectives and constraint conditions are determined, and the global optimal solution of parameterized mission area is explored by means of particle swarm optimization algorithm. Then the time-space weight of drift prediction data is defined, which will further increase the POS value of optimal mission area. Meanwhile, in order to study the optimization effects of adding time-space (TS) weight, the TS-CIS algorithm is further put forward by combining it with CIS algorithm. Finally, through a case simulation analysis, the optimization results of CIS algorithm, PSO algorithm, TS-CIS algorithm and TS-PSO algorithm in different time intervals are compared. The simulation results illustrate that the TS-PSO algorithm can explore the global optimal solution, and the average optimization result is significantly improved, which has high practical value.

The rest of this paper is organized as follows. The optimization objective and constraint condition of MSAR mission area planning and the specific application of PSO algorithm in this problem are given in Section II. Then the definition of the TS weight is given in Section III, and the TS-CIS algorithm and the TS-PSO algorithm are further put forward. In order to illustrate the improvement effects of the proposed algorithms, the helicopter MSAR decision support system is designed in Section IV, and the effects are verified via many case-simulation analyses. The last section concludes this paper and offers the future work.

II. MISSION AREA PLANNING WITH PSO ALGORITHM

As claimed by international aeronautical and maritime search and rescue manual [18], when a maritime distress warning is received, the chief thing that decision-makers should do is to obtain the distress location and time to predict drift trajectory [19]–[21]. When an object floats on the water surface without power, its drift condition is mainly affected by environmental factors such as surface wind and flow and its own factors such as immersion ratio and ballast condition [22]. Meanwhile, the calculation of wind-induced drift and flow-induced drift are influenced by uncertain factors. Therefore, the Monte Carlo method [23]–[25] is generally used in drift prediction and the Lagrange method [26]–[28] is used to constantly track the change of position. In this paper, drift prediction data provided by XiaMen LanHaitian Information Technology CO., LTD [29] is the basis of subsequent calculations. And its format is similar to the data provided by a lot of authoritative institutions [30], which is conducive to the practical application of the algorithm to be presented in following description.

After obtaining the drift prediction data, the decision-makers will filter the data within the required time interval based on SARU capabilities and then plan the mission area, which is a key link in formulating a helicopter MSAR response plan [31]. In order to find the optimal mission area, it is necessary to calculate the POS value in current mission area on the basis of the optimal search theory. Then, according to the boundary information of drift prediction data, the optimal mission area with the highest POS value can be searched by exploring the region parameters using optimization algorithm. It can be seen from the above argument that when determining the helicopter MSAR mission area, drift prediction is the data basis, probability calculation is its optimization objective, and the data boundary constrains the exploration of mission area. In addition, due to the rapid response capacity of helicopter, the mission area tends to be not very large. As a result, the longitude and latitude can be converted from spherical coordinate system to plane coordinate system, which is usually represented by the Mercator coordinates, within the margin of error.

A. OPTIMIZATION OBJECTIVE

The values of POC, POD and POS for a certain SARU in a mission area can be calculated based on the search theory [32]. When exploring optimal mission area, the optimization objective must make the POS value as large as possible, which needs to be comprehensively calculated from the POC of SART and the POD of SARU. In addition, parallel line search pattern is most commonly used in helicopter MSAR mission, as a result, the mission area discussed in this paper is a rectangular region.

1) POC CALCULATION

The location distribution of SART at different times can be found based on the drift prediction data. Because the helicopter MSAR mission is generally performed within a certain period of time, the prediction data from multiple consecutive prediction time points will be selected for analysis, which is usually expressed as discrete points. The POC value is always calculated based on the ratio of the number of points contained in the current mission area to the number of all points. Therefore, when the multiple discrete point sets corresponding to multiple time points, which is defined by $DD_{filtrate} = \{S_i | i \in [a, b]\}$, need to be considered, the POC value can be calculated as follows.

$$POC = \sum_{a}^{b} R_i \tag{1}$$

where a is the starting point of time, b is the ending point of time, $R_i = n(S_i')/n(S_i)$ is the coverage ratio of each set, and S_{ij}' is the set of drift prediction points in S_{ij} which is contained in the mission area.

2) POD CALCULATION

When the SARU searches in a certain rectangular region without knowing the specific information of targets, such as the location and movement, the random search method can be used. Then the POD value can be calculated as follows.

$$POD = 1 - \exp\left(-W \cdot V \cdot T / A\right) \tag{2}$$

where W is the sweep width of SARU, V is the search speed of SARU, T is the search time of SARU, A is the area of the rectangular region.

The POD value directly reflects the response capability of SARU to find the SART, which is mainly determined by its own flight performance and airborne equipment. According to the search theory set up by Koopman [33], [34], the search effort of SARU can be expressed as $Z = W \cdot V \cdot T$, while $C = Z/A$ can be taken to measure the effective coverage of SARU, which are the important references for decision-makers.

3) POS CALCULATION

When the POC value and the POD value are calculated, the POS value can be calculated as follows.

$$POS = POC \cdot POD \tag{3}$$

The POS value is a significant indicator for formulating and optimizing MSAR response plans, which means that the higher it is, the greater the probability that SART is successfully found and rescued by SARU in the mission area will be. It can be figured out from the calculation formulas of POS, POC and POD that when a specific SARU is selected to perform MSAR mission, the POC value increases and the POD value decreases with the area of rectangular region being larger, and vice versa. As a result, the maximum POS value can be found according to the parameter change of rectangular region, which provides a theoretical basis for the subsequent optimization algorithm of mission area.

B. CONSTRAINT CONDITION

In the process of exploring optimal mission area, it is necessary to calculate some important information of discrete

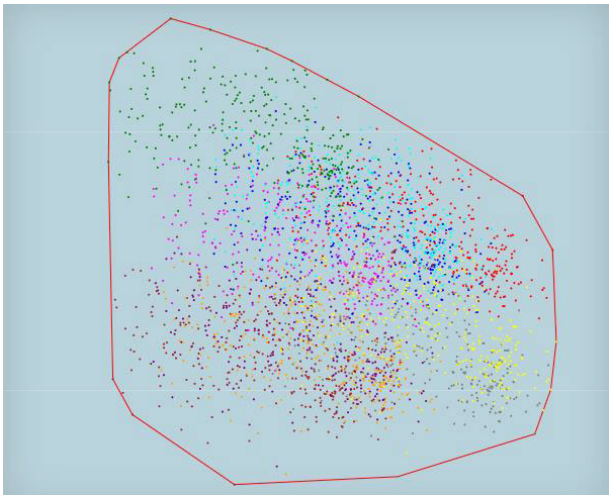

FIGURE 1. The MCB of discrete points.

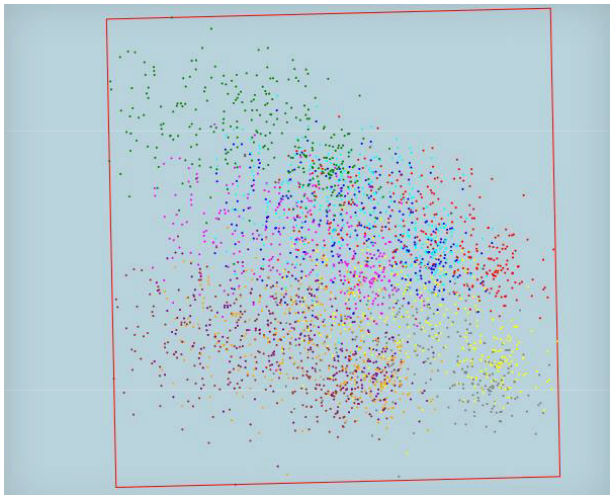

FIGURE 2. The MER of discrete points.

points corresponding to the drift prediction data, namely the minimum convex boundary (MCB) and the minimum enclosing rectangle (MER), which are the constraint conditions of optimization algorithm. The MCB and MER can be calculated as shown in Fig. 1 and Fig.2 when the drift prediction data is provided. It must be illustrated that multiple initial position of drift prediction calculation should be selected within a certain range near the alarm position, because the exact position of SART cannot be obtained accurately. In order to differentiate these data, the points with different color represent the simulation results of different initial positions.

1) MCB CALCULATION

The MCB of discrete points should be a convex polygon composed of boundary points. Therefore, MCB calculation means to find the boundary point set that makes up the convex polygon. The detailed processes are shown below:

Step 1: put all points in the Cartesian coordinate system and find the point with the largest ordinate and the smallest abscissa. Take this point as the initial point $P_0\,(x_0, y_0)$ and enter it into the boundary point set;

Step 2: assign $(x_0 - 1, y_0)$ to P_s and (x_0, y_0) to P_e;

Step 3: calculate the base vector $V_{base} = (P_e - P_s)$, which is the basis of each iteration;

Step 4: taking P_e as the rotation center and V_{base} as the starting vector, scan other points in clockwise direction to find certain point P_{next} with the smallest rotation angle;

Step 5: judge whether the point P_{next} is P_0. If not, put P_{next} into the boundary set and make $P_s = P_e$, $P_e = P_{next}$, then return to Step 3. Otherwise, continue to execute Step 6;

Step 6: output the closed curve that is connected with boundary points, which is the MCB.

The algorithm can find all vertices $C_{MCB}\,[n]$ of the MCB by continuously scanning and updating the reference vector when the discrete point set $C_{input}\,[n]$ is given. The flowchart and pseudocode of MCB are shown as Fig.3.

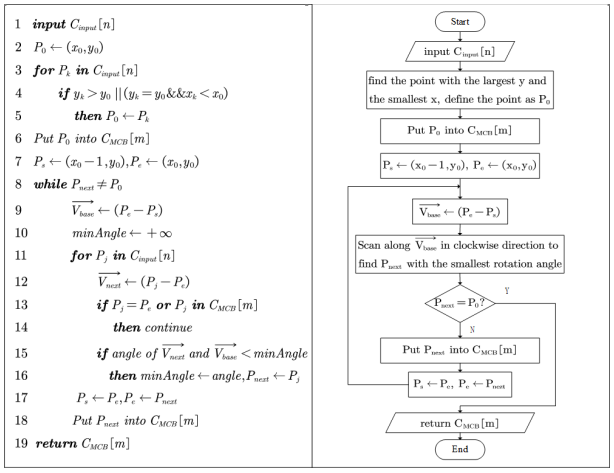

FIGURE 3. The flowchart and pseudocode of MCB.

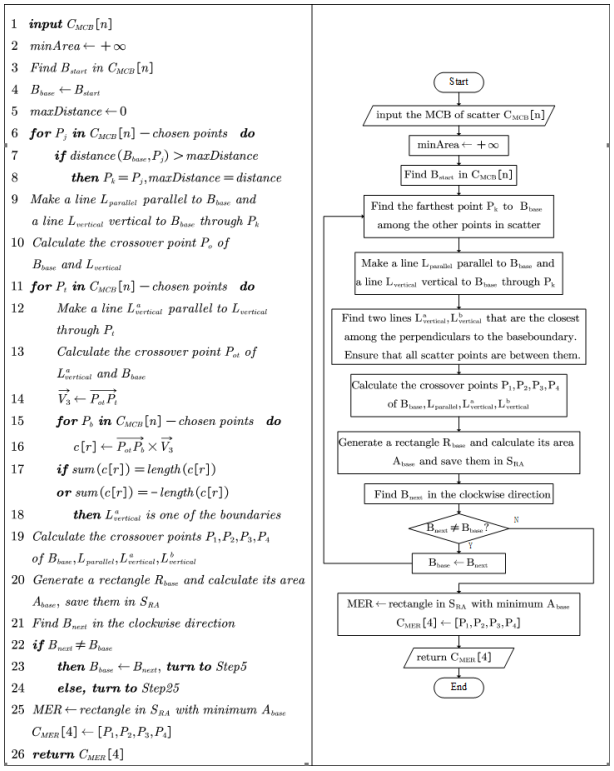

FIGURE 4. The flowchart and pseudocode of MER.

2) MER CALCULATION

Rotating Calipers method [35] is an algorithm that uses convexity to generate MER of any convex polygon. After the MCB of a calculated discrete point set is obtained, the MER of it can be calculated by this algorithm. The detailed processes are shown as follows:

Step 1: randomly select one edge of MCB as the starting boundary B_{start} and define it as the base boundary B_{base};

Step 2: find the farthest point among the other points and make a line $L_{parallel}$ parallel to base boundary;

Step 3: create two closest lines $L^a_{vertical}$ and $L^b_{vertical}$ perpendicular to base boundary, and ensure that all points are located between them. Then, calculate the four intersections P_1, P_2, P_3, P_4 of B_{base}, $L_{parallel}$, $L^a_{vertical}$ and $L^b_{vertical}$;

Step 4: generate a rectangle R_{base} using these four points in step 3 and calculate its area A_{base}. Then store R_{base} and A_{base} as key-value pairs into the set S_{RA};

Step 5: find another boundary B_{next} of MCB adjacent to the base boundary in clockwise direction. If $B_{next} \neq B_{start}$, make $B_{base} = B_{next}$ and return to Step 2. Otherwise, execute Step 6;

Step 6: find the rectangle in set S_{RA} with smallest area, which is MER of the scatter.

The algorithm can find all rectangle vertices $C_{MER}\,[4]$ of MCB boundaries and its area, then the rectangle with the smallest area can be found. The flowchart and pseudocode of MER are shown as Fig.4.

C. PSO ALGORITHM

Based on the optimization objective and constrain conditions mentioned above, the mission area can be planned using PSO algorithm. Considering that the mission area discussed in this paper is rectangular region, it can be defined by five parameters.

$$MA = [cLon, cLat, maL, maW, maA] \tag{4}$$

where $cLon$ represents the longitude of the rectangle center; $cLat$ represents the latitude of the rectangle center, maL represents the length of the rectangle, maW represents the width of the rectangle, maA represents the angle between the perpendicular of long side and the positive direction of horizontal axis.

As a result, to determine the mission area means to determine these 5 parameters. In addition, according to the optimal search theory, the optimization objective is maximizing POS value of mission area with constraint conditions, which can be expressed in (5).

$$\begin{aligned} &\max\ POS = POC \cdot POD \\ &s.t. \begin{cases} (cLon, cLat) \in A_{MCB} \\ maL \le L_{MER} \\ maW \le W_{MER} \\ maA \in [0, 2\pi] \end{cases} \end{aligned} \tag{5}$$

where A_{MCB} represents the inner region of MCB, L_{MER} represents the length of MER, W_{MER} represents the width of the MER.

It should be noted that the optimized POS value only shows relativeness among algorithms when comparing the results of them, which means it cannot represent the actual success probability of MSAR mission execution when discussed separately.

1) PARTICLE DEFINITION

a: POSITION AND VALUE RANGE OF PARTICLE

According to the parameterized definition of the mission area, the positions of particles obtained by each iteration can be expressed as follows.

$$X^i_{ma} = \left[X^i_{cLon}, X^i_{cLat}, X^i_{maL}, X^i_{maW}, X^i_{maA}\right]' \tag{6}$$

It can be seen from (3) that the POS value of the mission area is determined by the POC and POD value, which will be influenced by coupling effect of $cLon$, $cLat$, maL, maW and maA. Therefore, the fundamental work of PSO algorithm is to define the value range of each parameter.

$$\begin{cases} \left(X^i_{cLon}, X^i_{cLat}\right) \in A_{MCB} \\ X^i_{maL} \in \left[\sqrt{L_{MER} \cdot W_{MER}/5}, L_{MER}\right] \\ X^i_{maW} \in \left[\sqrt{L_{MER} \cdot W_{MER}/5}, W_{MER}\right] \\ X^i_{maA} \in [0, 2\pi] \end{cases} \tag{7}$$

The ranges shown in (7) are mainly determined based on the following analyses.

a. X^i_{cLon} and X^i_{cLat} determine the central location of the mission area. According to the analysis of optimization objective, the evolution trend of optimal mission area is to contain mor points and to maximize the coverage ratio of SARU. The first trend makes optimal mission area as large as possible, and the second makes it as small as possible. In conclusion, points defined by X^i_{cLon} and X^i_{cLat} are generally within MCB.

b. X^i_{maL} and X^i_{maW} determine the size and shape of the mission area. When considering only SART and ignoring the change of POD value, the optimal mission area is MER under the condition that the area is as small as possible while the POC value is as large as possible. When considering only SARU and ignoring the change of POC value, it is obvious that the smaller the mission area is, the greater the coverage ratio will be. Assuming that the SARU just completes a parallel line search in MER, then according to the correspondence between coverage ratio and POD value, the ratio of search effort to mission area should not be greater than 5 when the POD value is no more than 0.99, which means $\frac{L_{MER} \cdot W_{MER}}{X^i_{maL} \cdot X^i_{maW}} \le 5$. Therefore, under the condition of balancing the accuracy and computational efficiency as much as possible, the side length of square mission area is taken as the lower bound of these two parameters.

c. X^i_{maA} represents the angle between the vertical direction of the long side and the positive longitude direction. Therefore, each mission area corresponds to two angle values, and the value range should be $[0, \pi]$. However, if the range is shortened compulsorily, the PSO algorithm may cannot effectively cover all feasible solutions in iterative process. As a result, the range of X^i_{maA} is extended to $[0, 2\pi]$.

b: VELOCITIES OF THE PARTICLES

According to the basic definition of PSO algorithm, the velocities of particles in each iteration can be expressed as follow.

$$V^i_{ma} = \left[V^i_{cLon}, V^i_{cLat}, V^i_{maL}, V^i_{maW}, V^i_{maA}\right]' \tag{8}$$

The value of V^i_{ma} will be calculated according to the global optimal position and local optimal position, and it will be used for updating X^i_{ma}. As a result, its range is not limited. However, when the updated X^i_{ma} is beyond its range, the particle position should be performed out-of-range processing in order to restrict V^i_{ma} indirectly. These contents will be described in the following discussion.

2) PARAMETER UPDATING

For each particle, the updated formula of position and velocity can be obtained with the basis theories of PSO algorithm [36], [37], which is shown as follows.

$$\begin{aligned} V^i_{ma} &= \omega \cdot V^{i-1}_{ma} + c_g \cdot r^i_g \cdot D^i_{global} + c_p \cdot r^i_p \cdot D^i_{particle} \\ X^i_{ma} &= X^{i-1}_{ma} + V^i_{ma} \end{aligned} \tag{9}$$

where: V^i_{ma} is the velocity of particles at the i^{th} iteration, X^i_{ma} is the position of particles at the i^{th} iteration, ω represents the inertia factor for increasing the rate of convergence, $D^i_{global} =$

$X^i_{gbest} - X^i_{ma}$ is the vector from current particle's position to the global optimal position, $D^i_{particle} = X^i_{pbest} - X^i_{ma}$ is the vector from current particle's position to its local optimal position, c_g represents the global learning factor, c_p represents the local learning factor, r^i_g, r^i_p are five-dimension vectors and the value in each dimension is a random number with u (0, 1).

The value of ω determines both global optimization ability and local optimization ability. When it increases, the global optimization ability is strong and the local optimization ability is weak. While when it decreases, the relationship is reversed. However, the better optimal result can be obtained by dynamic ω, which could be changed linearly or dynamically according to certain measure function during the process of PSO algorithm exploration. Currently, the linear decreasing weight (LDW) [38] strategy as follows is widely applied.

$$\omega_i = (\omega_{ini} - \omega_{end}) \cdot (G_k - g) \big/ G_k + \omega_{end} \tag{10}$$

where G_k represents the maximum number of iterations, ω_{ini} represents the initial inertia weight, ω_{end} represents the maximum inertia weight.

3) OUT-OF-RANGE PROCESSING

a: OUT-OF-RANGE PROCESSING OF X^i_{cLon} AND X^i_{cLat}

These two parameters are highly correlated and cannot be processed independently. As a result, they must be further updated together when the central point of mission area generated after each iteration is not within the MCB. Suppose that the central point of mission area in $i-1$ iteration is P_{i-1} in MCB, and the point in i^{th} iteration is P_i beyond the limit of MCB, then the central point of mission area in i^{th} iteration could be set as the intersection point of $\overline{P_{i-1}P_i}$ and MCB.

b: OUT-OF-RANGE PROCESSING OF X^i_{maL}, X^i_{maW} AND X^i_{maA}

These three parameters have little correlation and can be processed independently. When these parameters calculated in i^{th} iteration is out of their ranges, the nearest boundary value will be taken. In another words, the minimum boundary value is taken when the parameter value is less than the minimum value, and the maximum boundary value is taken when the parameter value is greater than the maximum value.

4) OPTIMAL MISSION AREA ITERATIVE EXPLORATION

The optimal mission area can be explored iteratively after the above preparations. The termination condition of iterative exploration is that when the set number of iterations is reached or the variation of global optimal fitness is less than ε in continuous n times. The detailed processes of PSO algorithm are expressed as follows.

Step 1: initialize the position of each particle according to parameter range, and define the velocity as 0;

Step 2: calculate the fitness of each particle and initialize the local optimum and global optimum;

Step 3: update the velocity, position and fitness;

Step 4: calculate current local optimal fitness value and local optimal solution;

Step 5: calculate current global optimal fitness value and global optimal solution;

Step 6: judge whether the termination conditions are satisfied. If not, return to Step 3. Otherwise, continue to execute Step 7;

Step 7: output current global optimal solution as the optimal mission area of the PSO algorithm.

The process to search the optimal mission area of the discrete points with PSO algorithm is shown in Fig.5, where a) shows the initial mission area, b) shows the solution after 5^{th} iterations, c) shows the solution after 10^{th} iterations, and d) shows the optimal mission area. In each iteration, the regions with green boundary are mission areas corresponding to each particle, while the regions with blue boundary is the global optimal mission area in current iteration.

D. COMPARISON OF THE CIS ALGORITHM AND THE PSO ALGORITHM

This paper takes a helicopter MSAR mission of searching for the missing people fallen off a sunken fishing boat on July 2, 2018 as reference. The initial drift prediction locations is located a circular region, the central position is (E118°30', N023°22') and the radius is 5km. In addition, the probabilities of the initial locations follow a uniform distribution. Ten initial locations are randomly selected in this region and the drift prediction data within one day is calculated. Assuming that the simulation start time is 0 and the data is predicted every one hour, then there are 24 groups of data, which is used as the time index for filtering.

All drift prediction data are divided into 4 time-intervals to be discussed. The optimization results of CIS algorithm and PSO algorithm are analyzed as shown in Fig.6. As the theoretical definition of CIS algorithm, its results are mainly related to the grid quantity, while the results of PSO are primarily influenced by the particle quantity. As a result, the grid quantity within [50,1000] and the particle quantity within [5,100] are respectively taken for analyses. In order to discuss the variation pattern clearly, the data is fitted to $f(x) = a \cdot x^b + c$ with 95% confidence interval and represented by a solid line.

According to the data in Table. 1 and the mathematical properties of the fitted curve, c is the extreme value of the corresponding curve. Therefore, for the CIS algorithm, c value is the POS value of optimal mission area when grids quantity is positive infinity, while for the PSO algorithm, c value is the POS value of the optimal mission area when particles quantity is positive infinity. Consequently, the extreme value can be taken as an objective scale for the calculation results of these two algorithms.

It can be seen from above that the optimization results of the PSO algorithm are obviously better than that of the CIS algorithm when exploring the optimal mission area in these four periods. The main reason is that the PSO algorithm takes the parameterized definition of mission area as basis,

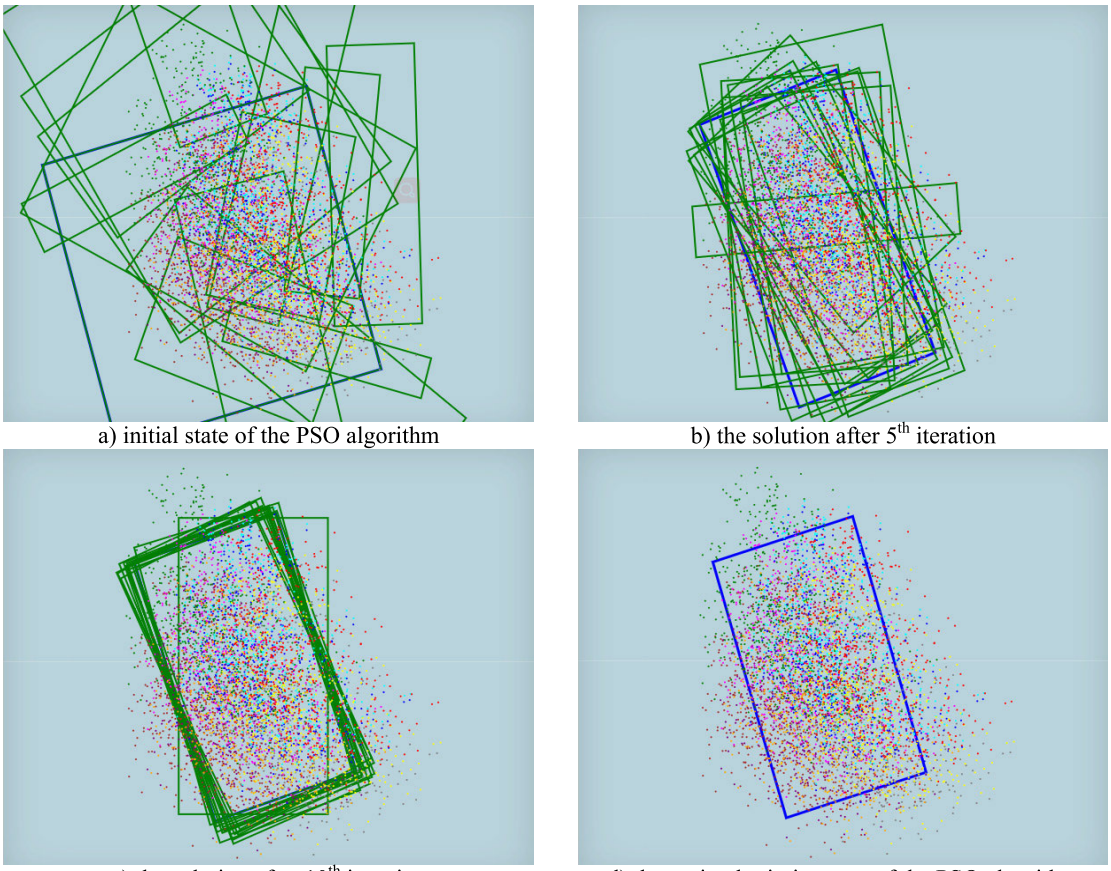

a) initial state of the PSO algorithm
b) the solution after 5th iteration
c) the solution after 10th iteration
d) the optimal mission area of the PSO algorithm

FIGURE 5. The optimization process of the PSO algorithm.

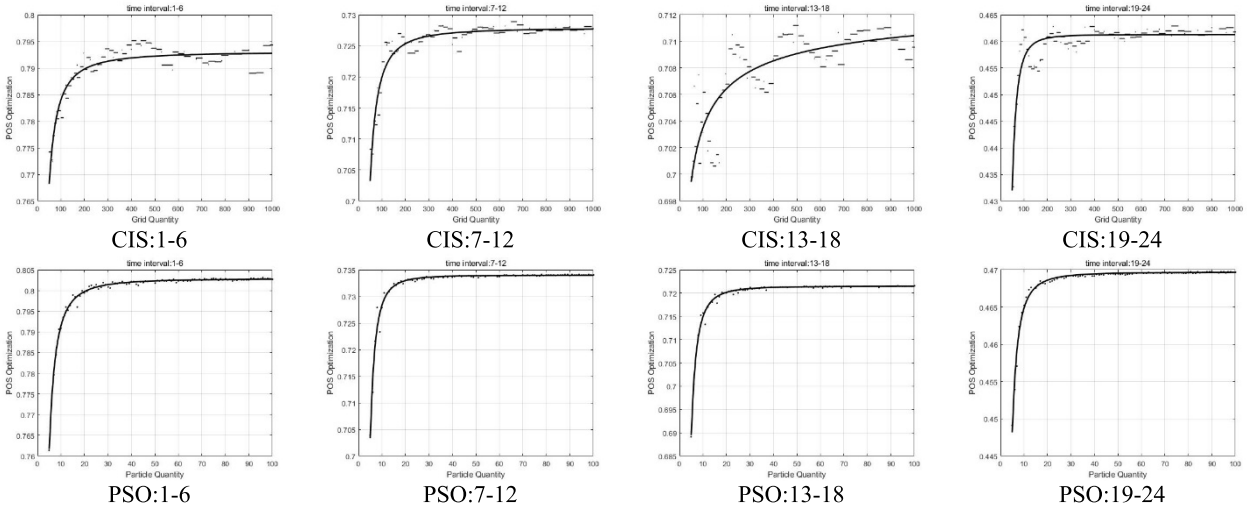

FIGURE 6. The optimization results of the CIS algorithm and the PSO algorithm.

which is able to explore any combination conditions of all dimensions within the value range of parameters. In addition, the value of each dimension can be equal to any value in its range according to the velocity and position updating process of the PSO algorithm, which can be regarded as continuous optimization process. Therefore, the PSO algorithm makes up for the shortcoming that the CIS algorithm is often trapped in the local optimal solution, and can make the optimization result converge to global optimal solution as much as possible.

TABLE 1. The fitting results of the CIS algorithm and the PSO algorithm.

Algorithm	Time	a	b	c	SSE	S-square
CIS	01-06	-7.496	-1.459	0.7931	0.002957	0.8034
	07-12	-14.90	-1.637	0.7279	0.001355	0.8885
	13-18	-0.094	-0.477	0.7139	0.002275	0.6742
	19-24	-1221	-2.719	0.4613	0.002722	0.7741
PSO	01-06	-0.816	-1.855	0.8029	2.551e-5	0.9925
	07-12	-1.581	-2.450	0.7340	3.527e-5	0.9784
	13-18	-1.279	-2.291	0.7215	1.921e-5	0.9896
	19-24	-0.689	-2.153	0.4697	1.102e-5	0.9873

III. MISSION AREA PLANNING BASED ON TS WEIGHT

A. TIME-SPACE WEIGHT DEFINITION

In actual helicopter MSAR missions, the distress position reported by SART is generally inaccurate due to systematic errors. As a result, the initial position of drift prediction can be considered in a primary area (PA) which follows a certain two-dimensional probability distribution. At the same time, because of the accumulated error of drift prediction algorithm, the data accuracy decreases gradually with prediction time increasing. Therefore, it is necessary to solve these problems before planning MSAR mission area, which is called the TS weight issue in this paper.

1) TIME WEIGHT

Assuming that the drift prediction result includes data from N_t time points, and the reliability of data at i^{th} predicted time after the initial simulation time will be $C_i = aa^i$, where aa is the accuracy of drift prediction algorithm. If the mission area will be optimized based on the drift prediction data in the period of time from a to b, the time weight W_T^i of drift prediction data can be expressed as follows.

$$W_T^i = C_i \Big/ C_{total}, \quad i \in [a, b] \tag{11}$$

where $C_{total} = \sum_a^b C_i$, i is each predicted time, a, b mean integers relative to the starting time of drift prediction.

2) SPACE WEIGHT

Assuming that the probability distribution function of actual initial location in PA is $F\ (lon, lat)$ and the probability density function is $f\ (lon, lat)$, then the specific relationship is shown as follows.

$$F\ (lon, lat) = \oiint_{PA} f\ (lon, lat) d_{lat} d_{lon} \tag{12}$$

When N_s initial positions are selected randomly, the probability density of j^{th} initial position is P_s^j, and the space weight W_s^j of drift prediction data can be expressed as follows.

$$W_s^j = P_s^j \Big/ P_{total}, \quad j \in [1, N_s] \tag{13}$$

where $P_s^j = f\left(lon^j, lat^j\right), \left(lon^j, lat^j\right) \in PA$, j represents each initial position, $P_{total} = \sum_1^{N_s} P_s^j$ represents the sum of all probability density.

3) TS WEIGHT

Assuming that the discrete point set of j^{th} initial position at i^{th} predicted time is S_{ij}, then the TS weight W_{TS}^{ij} of it can be expressed as follows.

$$W_{TS}^{ij} = \left(W_T^i + W_S^j\right) \Big/ W_{TS}^{total} \tag{14}$$

where $W_{TS}^{total} = \sum_{i=1}^{N_t} \sum_{j=1}^{N_s} W_T^i + W_S^j$ represents the sum of time weights and space weights.

Furthermore, the weighted data set filtered by the capability of SARU can be expressed as $DD_{filtrate}$ through drift prediction and TS weight calculation. It represents the corresponding relationship between each discrete point set S_{ij} and its TS weight W_{TS}^{ij}.

$$DD_{filtrate} = \left\{ S_{ij} : W_{TS}^{ij} | i \in [x, y], j \in [1, N_s] \right\} \tag{15}$$

where $b - a + 1 = N_t$.

B. ALGORITHM IMPROVEMENT BASED ON TS WEIGHT

Through the above detailed analysis of these specific characteristics of drift prediction data, it can be figured out that the TS weight further considers the uncertainty of data calculated by drift prediction algorithm. With these worthy considerations, the predicted position probability of SART is closer to the actual distribution to some extent. The calculation method of POC is reorganized on this basis, in addition, the TS-CIS algorithm and TS-PSO algorithm are further proposed in the following parts.

1) POC CALCULATION WITH TS WEIGHT

Taking TS weight of drift prediction data into consideration, the POC value can be calculated as follows.

$$POC = \sum\nolimits_{DD_{contain}} R_{ij} \cdot W_{TS}^{ij} \tag{16}$$

where $DD_{coverage} = \left\{ S'_{ij} : W_{TS}^{ij} | S'_{ij} \in DD_{filtrate} \right\}$ represents the contained data set and its corresponding TS weight, $R_{ij} = n(S'_{ij}) \Big/ n(S_{ij})$ represents the coverage ratio of filtered data set S_{ij}, S'_{ij} represents the subset of S_{ij} which is covered by mission area.

2) TS-CIS ALGORITHM

The POC value is usually calculated by classical CIS algorithm without TS weight, which considers the SART appearing with equal probability in the predicted position. Therefore, the TS-CIS algorithm is proposed in this paper on the basis of (16). The optimization procedure of this algorithm mainly includes two parts, grid partition and optimal mission area iterative extension.

a: GRID PARTITION

According to the basic process of the CIS algorithm, grid partition of the MER should be completed firstly in the TS-CIS algorithm, because it will influence the calculation of POC value. There are two main methods of grid partition, namely dividing with fixed grid length and fixed grid quantity, while both of them need to adjust the distribution of grid according to the actual situation. Suppose that nL is the actual number of long-side grids, nW is the actual number of short-side grids, L_{Grid} is the length of actual grid long-side, W_{Grid} is the length of actual grid short-side, C_{AG} is the center position of the rectangle formed with all grids, N_{Grid} is the actual grid quantity.

When grids are divided with fixed grid length L^0_{Grid} and W^0_{Grid}, the length and width of MER are generally not the integral multiples of grid length. The following relationship of nL, nW and C_{AG} must be satisfied.

$$\begin{aligned} L^0_{Grid} \cdot (nL-1) &\le L_{MER} \le L^0_{Grid} \cdot nL \\ W^0_{Grid} \cdot (nW-1) &\le W_{MER} \le W^0_{Grid} \cdot nW \\ C_{AG} &= C_{MER} \end{aligned} \tag{17}$$

where C_{MER} represents the position of the MER center. $N_{Grid} = nL \cdot nW$ represents the actual grid quantity.

When grids are divided with fixed grid quantity N^0_{Grid}, the length-width ratio of MER generally does not meet the requirement of grid quantity. The following relationship of nL, nW must be satisfied, by which $L_{Grid} = L_{MER}/nL$ and $W_{Grid} = W_{MER}/nW$ can be calculated.

$$\begin{aligned} \frac{nL-1}{N_{Grid}/(nL-1)} < \frac{L_{MER}}{W_{MER}} &\le \frac{nL}{N_{Grid}/nL} \\ nW &= nL \cdot \frac{L_{MER}}{W_{MER}} \end{aligned} \tag{18}$$

It is necessary to illustrate that the specific way of grid partition must be selected according to actual conditions. The accuracy and efficiency of algorithm must be ~~integrated~~ considered integrally, and the appropriate way can be selected according to the range of drift prediction data. Meanwhile, a two-dimensional vector (RP_L, RP_W) is used to represent the relative position of certain grid in all grids so that the following iterative extension process can be executed more conveniently. And the RP_L means the position serial number in L_{MER} direction, while RP_W is the position serial number in W_{MER} direction. After the grid partition is completed, the POC value of each grid can be calculated and the grid with the largest POC value will be selected as the initial region of the TS-CIS algorithm.

b: OPTIMAL MISSION AREA ITERATIVE EXTENSION

In the extension process, a rectangular region will be obtained in each iteration of the TS-CIS algorithm, because the optimal mission area, the MER and each grid are all rectangular areas. The detailed processes of optimal mission area iterative extension are expressed as follows.

Step 1: define the initial region as the base region R_{base} and calculate the corresponding POD value and POS value.

Step 2: extend R_{base} in four relative directions $(-1, 0)$, $(0, +1)$, $(+1, 0)$ and $(0, -1)$. Then four new rectangular regions $R_{(-1,0)}$, $R_{(0,+1)}$, $R_{(+1,0)}$, $R_{(0,-1)}$ can be obtained;

Step 3: calculate the corresponding POC, POD and POS value of each new rectangular region;

Step 4: define the region with the maximum POS value as R_{MAX}, and compare this POS value with that of R_{base}. If the former is bigger, make $R_{base} = R_{MAX}$ and return to Step 2. Otherwise, continue to execute Step 5;

Step 5: output R_{base} as the optimal mission area of TS-CIS algorithm.

The process to search the optimal mission area of the discrete points with TS-CIS algorithm is shown in Fig.7, where a) shows the initial region of TS-CIS, b) and c) give the results after the first and the seventh extension, and d) shows the optimal mission area obtained by TS-CIS algorithm. In each iteration, the red region is R_{base}, the orange region is $R_{(-1,0)}$, the green region is $R_{(0,+1)}$, the blue region is $R_{(+1,0)}$, the purple region is $R_{(0,-1)}$.

It must be figured out that the MER and corresponding grid partition result limit the ability of CIS algorithm to explore optimal mission area. Under this influence, the value of maA must be the long side direction or the short side direction of MER, the value of maL and maW must be integral multiple of the grid side length. the value of $cLon$ and $cLat$ are both associated with the location of output R_{base} and each grid. Therefore, through the comparative analysis of two algorithms, an important conclusion can be drawn that CIS algorithm can only find the local optimal solution, while PSO algorithm can obtain the global optimal solution, which further proves the comparative conclusions of these two algorithms from a theoretical point of view.

3) TS-PSO ALGORITHM

Combined with the discussion of PSO algorithm, the TS weight of drift prediction data will change the POC calculation method in each iteration, and consequently change the calculation result of particle fitness. Therefore, TS-PSO algorithm is further proposed in this paper. The main flow of the algorithm is the same as that described in detail in previous section, and only the calculation method of particle fitness is promoted. In this way, it is convenient to discuss the improvement effects of TS weight on different optimization algorithms results.

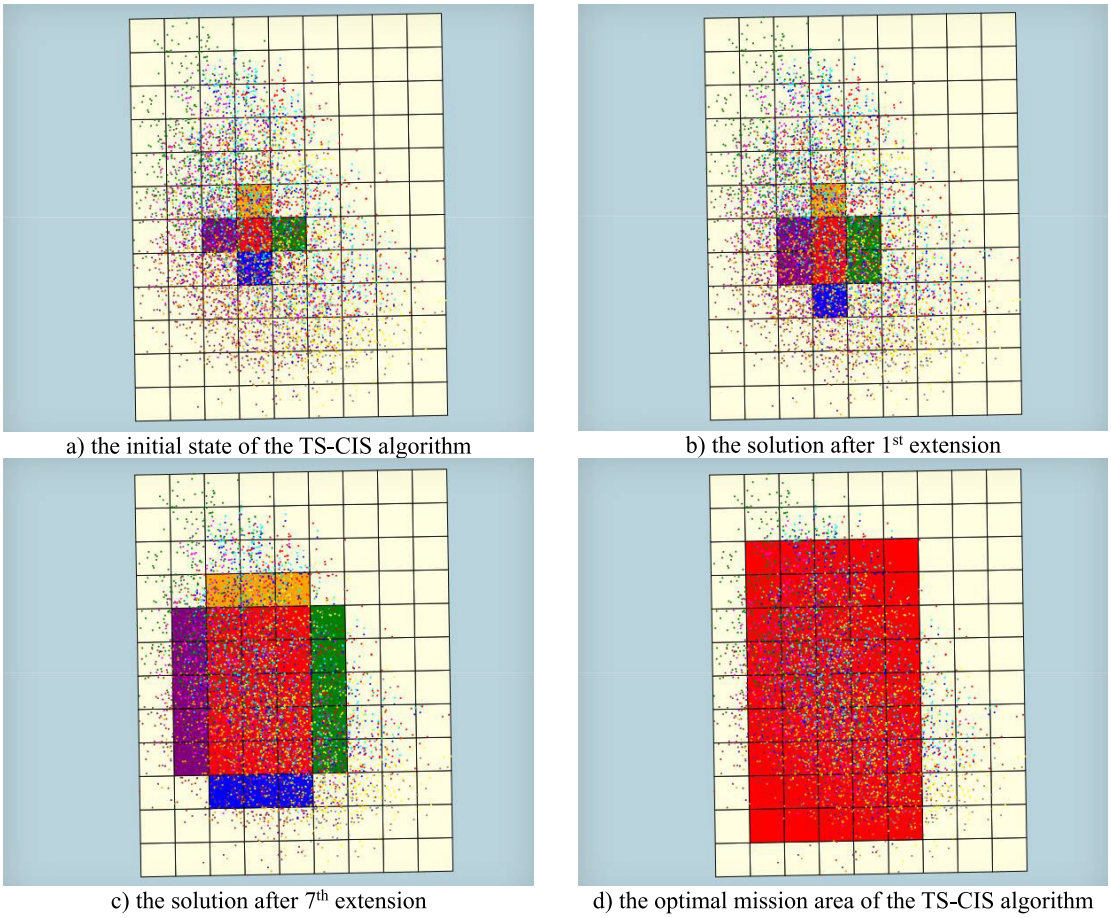

FIGURE 7. The optimization process of TS-CIS algorithm.

IV. CASE SIMULATION ANALYSIS

In order to comparatively analyze these two algorithms and apply them to actual mission more conveniently, the helicopter MSAR decision-making system has been designed based on above theoretical methods, the system interface is shown in Fig.8. The gray rectangle boxes respectively contain SART editing, SARU editing and drift prediction, which are not the focus of this paper, so they are not discussed. The green rectangle box represents the drift data processing, it mainly includes the methods described in constraint conditions and time-space weight of drift prediction data. The yellow rectangle boxes refer to the comparative analysis and validation, which mainly includes the methods described in TS-CIS algorithm and TS-PSO algorithm. The upper right of system interface is the display window of the algorithm execution results, in which the cyan solid convex polygon is MCB, the purple solid rectangle is MER, the blue rectangle is the optimal mission area obtained by TS-CIS algorithm, and the red rectangle is the optimal mission area obtained by TS-PSO algorithm.

A. ANALYSIS OF TS-CIS ALGORITHM

The final result of TS-CIS algorithm is closely related to grid division based on the description of it. However, more information is needed to determine the specific length of the grid based on fixed grid length. In order to improve the practicability, this paper chooses to divide the grid based on the fixed grid quantity. Therefore, the influence of the grid quantity on POS value, run-time and iteration of TS-CIS algorithm have been analyzed with or without TS weight. Take the grid quantity as [50,1000], and divide the prediction data within 1 day into 4 groups for discussion.

Fig.9 shows the relationship between the grid quantity and the POS value, where the red scatter is the output data when TS weight is considered, and the blue scatter is the output data when TS weight is not considered. Take the fitting curve analysis method as reference, the data is fitted to $f(x) = a \cdot x^b + c$ with 95% confidence interval, which is represented as a solid line with corresponding color. The fitting results are shown in Table.2.

It can be seen that the optimization result of TS-CIS algorithm is significantly higher when TS weight is considered than the case it is not considered. And the slope of the fitting curve decreases greatly when the grid quantity is greater than 300. In other words, the improvement effect of the grid quantity on the POS value is significantly reduced.

As shown in Fig.10, the red scatter is the result of considering the TS weight, and the blue scatter is the result of not

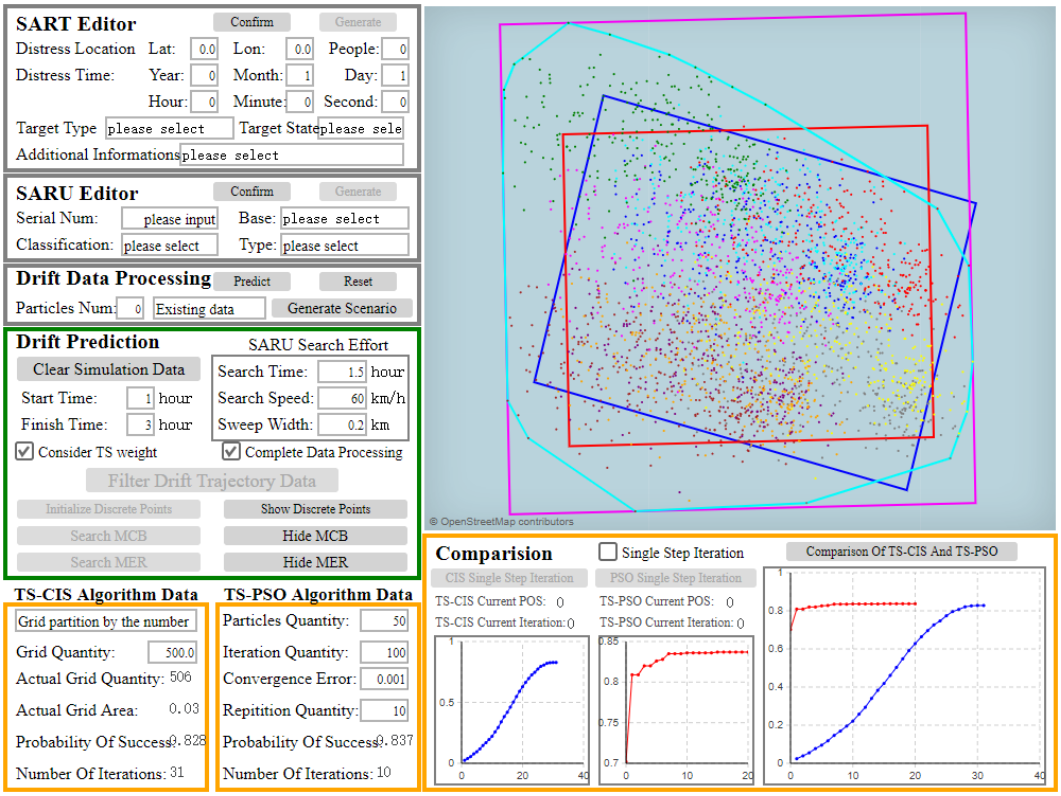

FIGURE 8. The user interface of helicopter MSAR decision support system.

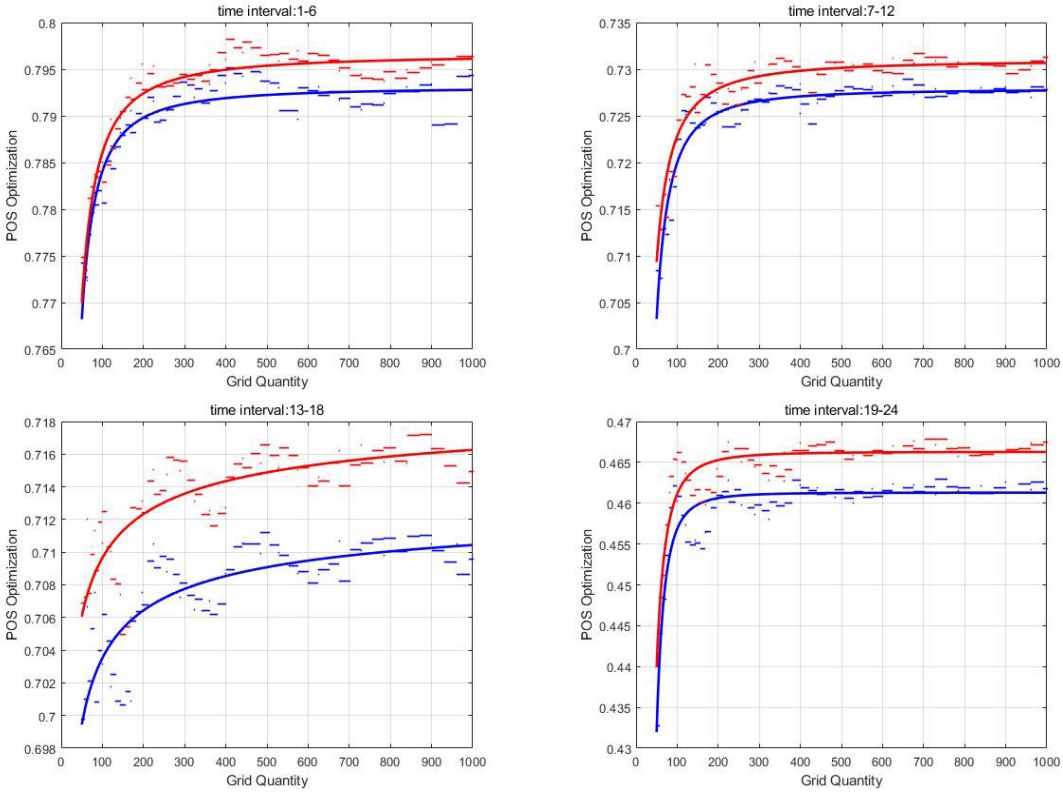

FIGURE 9. Accuracy analysis of TS-CIS algorithm.

TABLE 2. Fitting results of relationship between grid quantity and POS value.

TS-Weight	Time	a	b	c	SSE	S-square
Excluding	01-06	-7.496	-1.459	0.7931	0.002957	0.8034
	07-12	-14.90	-1.637	0.7279	0.001355	0.8885
	13-18	-0.094	-0.477	0.7139	0.002275	0.6742
	19-24	-1221	-2.719	0.4613	0.002722	0.7741
Including	01-06	-4.983	-1.337	0.7966	0.001940	0.8838
	07-12	-5.257	-1.404	0.7310	0.001573	0.8558
	13-18	-0.073	-0.415	0.7204	0.002494	0.6294
	19-24	-257.5	-2.348	0.4663	0.002435	0.7824

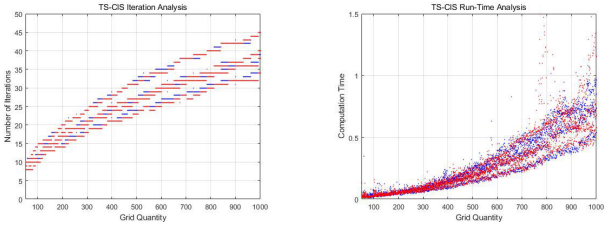

FIGURE 10. Efficiency analysis of TS-CIS algorithm.

considering the TS weight. It can be seen that TS weight has little impact on the number of iterations, but when the number of grids is greater than 500, the run-time increases greatly. Therefore, considering the performance of TS-CIS algorithm, a better effect can be achieved when the grid quantity is about 500.

B. ANALYSIS OF TS-PSO ALGORITHM

The final result of TS-PSO algorithm is closely related to particle quantity based on the description of it. Therefore, the influence of the particle quantity on POS value, run-time and iteration of TS-CIS algorithm have been analyzed with or without TS weight. Meanwhile, different initial states of particles will lead to different optimal results, which is determined by basic theory of PSO algorithm. As a result, in the case of the same particle quantity, the TS-PSO algorithm runs independently 100 times to obtain the average influence law, and the stability can be analyzed.

Fig.11 shows the relationship between the particle quantity and the POS value, where the red scatter is the output data when TS weight is considered, and the blue scatter is the output data when TS weight is not considered. The data is fitted to $f(x) = a \cdot x^b + c$ with 95% confidence interval as well, which is represented as a solid line of the corresponding color. The fitting results are shown in Table.3.

It can be seen that the optimization result of TS-PSO algorithm is significantly higher when TS weight is considered than the case it is not considered. And the slope of the fitting curve decreases greatly when the particle quantity is greater than 20. In other words, the improvement effect of the particle quantity on the POS value can be neglected. It is important to illustrate that the success ratio is defined to discuss the stability of TS-PSO algorithm. Suppose that the j^{th} calculation of i^{th} particle quantity is POS_i^j, then the success ratio SR_i can be obtained by equation shown as follows.

$$SR_i = n_{j=1}^{100}\left(d_i^j \geq (\max POS_i - \min POS_i)\cdot CL\right)\Big/100$$
$$\begin{cases} d_i^j = POS_i^j - \min POS_i \\ \min POS_i = \min(POS_i^j) \\ \max POS_i = \max(POS_i^j) \end{cases} \tag{19}$$

where $\max POS_i$ represents the max value of POS when particle quantity is i, $\min POS_i$ represents the min value of POS when particle quantity is i, $CL \in (0, 1)$ represents the confidence level, $n(\cdot)$ represents the number of simulation times satisfying the internal conditions.

As shown in Fig.12, when the particle quantity is more than 30, each simulation will converge to less than 5% of the total error from all simulation results with more than 90% probability, which satisfies the stability in practical application. On the other hand, as shown in Fig.13, the inflection point of the iteration occurs when the particle quantity is more than 50, while the run-time tends to diverge when the particle quantity is more than 60. Therefore, considering the performance of TS-PSO, a better effect can be achieved in practical application when the particle quantity is greater than 50.

C. COMPARISON OF THE TS-CIS ALGORITHM AND THE TS-PSO ALGORITHM

The values of c in different situations are shown in Fig.14. It can be seen that the optimal POS value decreases with the increase of drift time, indicating that the shorter the response time of SARU is, and the higher the POS value of helicopter MSAR mission will be. This relationship satisfies the objective law of MSAR mission, which indirectly demonstrates the rationality of above two algorithms. The further analysis of the POS promotion degree can be seen in Table.4, which illustrates that the TS weight will promote the optimal POS value of each algorithm, while TS-PSO algorithm improves the classical CIS algorithm more obviously.

D. COMPARISON FOR DIFFERENT SARUS

The TS-PSO algorithm proposed in this paper solves the problem of helicopter MSAR mission area planning. In order to discuss its universality, the situation that helicopter, fixed-wing aircraft and ship search and rescue drowning person

TABLE 3. Fitting results of relationship between particle quantity and POS value.

TS-Weight	Time	a	b	c	SSE	S-square
Excluding	01-06	-0.816	-1.855	0.8029	2.551e-5	0.9925
	07-12	-1.581	-2.450	0.7340	3.527e-5	0.9784
	13-18	-1.279	-2.291	0.7215	1.921e-5	0.9896
	19-24	-0.689	-2.153	0.4697	1.102e-5	0.9873
Including	01-06	-0.798	-1.914	0.8060	1.966e-5	0.9927
	07-12	-1.163	-2.324	0.7374	1.289e-5	0.9905
	13-18	-2.194	-2.576	0.7270	1.512e-5	0.9924
	19-24	-0.460	-1.913	0.4763	1.942e-5	0.9788

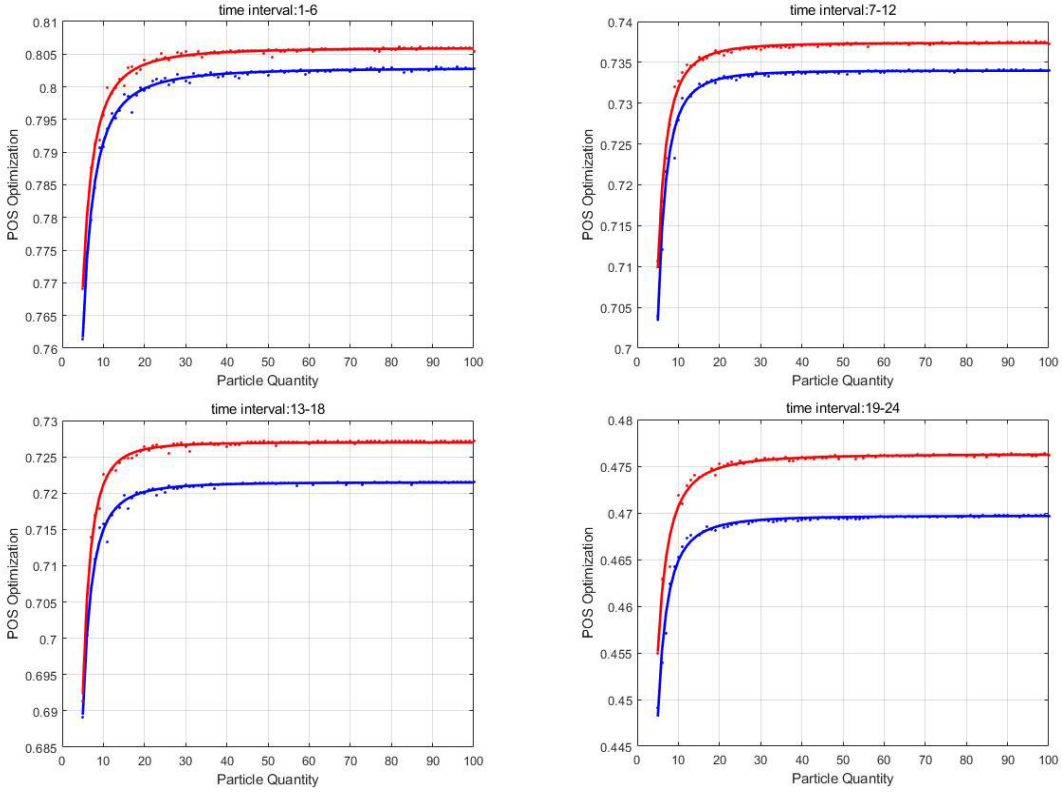

FIGURE 11. Accuracy analysis of TS-PSO algorithm.

is discussed, and the search efforts of different SARUs are shown in Table.5. According to the results of the performance analysis mentioned above, the TS-CIS algorithm with a grid quantity of 500 and TS-PSO algorithm with a particle quantity of 50 are selected, and the single POS values of these SARUs in different time interval are shown in Table.6. It should be noted that when the actual search time is greater than the search effort of SARU, the latter shall prevail.

In order to illustrate the improvement effect of TS-PSO algorithm more clearly, the data of same case in different algorithms are further analyzed and shown in Table.7. The results show that the TS-PSO algorithm can effectively improve the POS value in any case of different SARU under different time interval.

TABLE 4. Promotion degree of extremum under different conditions.

Time	TS to TS-CIS	TS to TS-PSO	PSO to TS-CIS	TS-PSO to CIS
01-04	0.98%	0.94%	0.63%	1.29%
05-08	0.61%	0.64%	0.30%	0.95%
09-12	0.76%	0.66%	0.11%	1.31%
13-16	0.84%	1.00%	0.34%	1.50%

E. DISCUSSION

According to the above analysis, it can be seen that both the TS-PSO algorithm and the TS-CIS algorithm can effectively improve the optimization result of the classical CIS algorithm in the mission area planning problem, and the former has

TABLE 5. Search effort of different SARU.

Search effort	Helicopter	Fix-wing	Vessel
Search time (h)	2	4	15
Search speed (km/h)	100	150	60
Sweep Width(km)	0.2	0.2	0.7

TABLE 6. The optimization results of two algorithm.

Algorithm	Time	Helicopter	Fix-wing	Vessel
TS-CIS	2	0.905454	0.956524	0.804493
	4	0.704531	0.944196	0.751357
	12	0.596598	0.849989	0.854143
TS-PSO	2	0.918818	0.964939	0.829074
	4	0.733563	0.950328	0.780092
	10	0.608268	0.854143	0.877672

TABLE 7. Promotion degree of the TS-PSO algorithm.

Time	Helicopter	Fix-wing	Vessel
2	1.48%	0.88%	3.06%
4	4.12%	0.65%	3.82%
12	1.96%	0.49%	2.75%

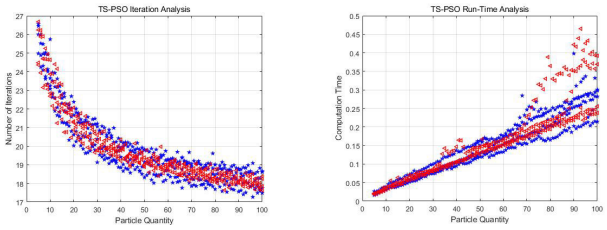

FIGURE 12. Efficiency analysis of TS-CIS algorithm.

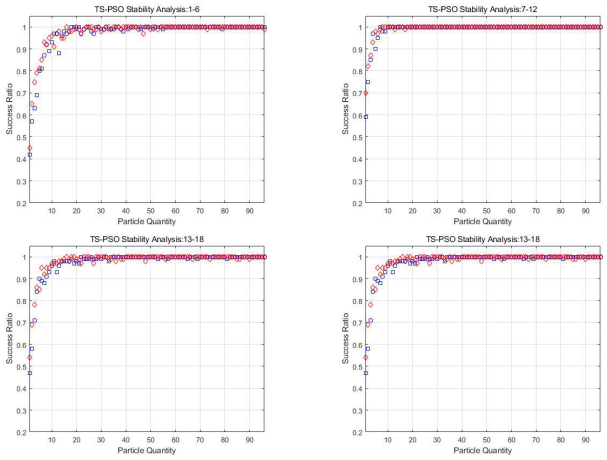

FIGURE 13. Stability analysis of TS-PSO algorithm.

higher stability, faster convergence speed and shorter runtime. However, the proposed algorithms have some limitations and disadvantages. The drift prediction is the basis of this algorithm, so the optimization result is highly dependent on the accuracy of it, that is, the more accurate the drift prediction data is, the more reliable the optimization result is. In addition, the time weight can only be calculated when the accuracy of drift prediction algorithm is known, while the space weight can only be calculated when the probability distribution of the initial position is known. Therefore, the application of the TS weight will be greatly affected in the decision-making support of actual helicopter MSAR mission.

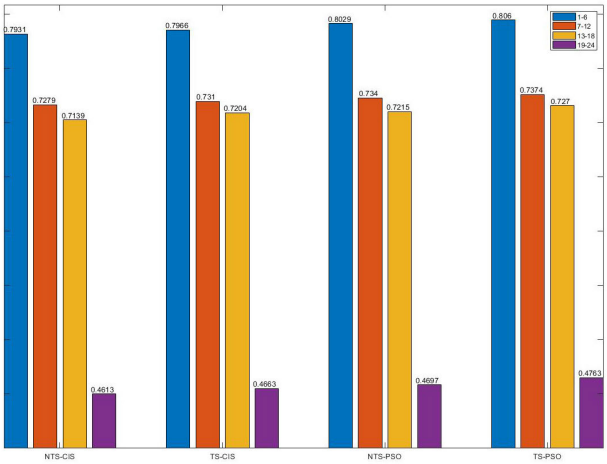

FIGURE 14. Relationship between extremum of different algorithm and time interval.

V. CONCLUSION

1. Aiming at the problem that the CIS algorithm is easy to fall into the local optimal solution when determining MSAR mission area, the TS-PSO algorithm is proposed in this paper. It can fully explore the definition domain of mission area parameters on the basis of analyzing the TS weight of drift prediction data, and then the global and greater optimal solution will be obtained.

2. The theoretical calculation process and optimization termination criterion of the TS-CIS and the TS-PSO are given. It can be seen that the input parameter of the former is grid distribution, and that of the latter is particle quantity. In addition, according to the theoretical characteristics of these two algorithms, the TS-CIS algorithm only calculates the local optimal solution due to the limitation of MER, while the TS-PSO algorithm can obtain the global optimal solution.

3. Through the analysis of the examples, it can be seen that the TS weight can improve the optimization results of both the TS-CIS algorithm and the TS-PSO algorithm, but the improvement effect is small. In comparison, the TS-PSO algorithm can improve the optimization result of the TS-CIS algorithm in all cases, and the improvement effect is relatively obvious. Therefore, it can be illustrated that the TS-PSO algorithm can not only explore the global optimal solution in the domain of parameterized mission area, but also its optimization result is significantly higher than the CIS algorithm, which proves the effectiveness and practicability of the TS-PSO algorithm sufficiently.

4. Moreover, there are many further works can be done. This paper discusses the application of the TS-PSO algorithm in the MSAR rectangular mission area planning, which corresponds to the area-datum search pattern. Then it can also be applied to the planning problem of point-datum search pattern and line-datum search pattern taking the parameterization method of rectangular mission area as a reference. At the same time, in order to illustrate the problem more intuitive, the single-helicopter-single-flight search process is discussed in this paper. However, the TS-PSO algorithm can also be extended to multi-helicopter-multi-flight search process according to the basic principle of algorithm and the data format of drift prediction. Another important problem is that the initial state of particle swarm has a great influence on optimization result and convergence rate, therefore, the relationship between them can be studied through design of experiment (DoE). These issues will be continuously carried out in the follow-up researches. Meanwhile, since the search theory can also be applied to land search and rescue (LSAR) [39] field, the TS-PSO algorithm mentioned in this paper and the follow-up scientific research achievements can also be applied to this field.

In this paper, according to the general procedure of PSO algorithm, a lot of improvement measures of the TS-PSO algorithm on the CIS algorithm are discussed from two perspectives, the search theory and the nature of drift prediction data. Then the improvement effect is adequately proved by comparison of theoretical calculation processes and case simulation analysis. Thereby the optimal mission area of different SARU in different time intervals can be obtained by this algorithm, and then the helicopter MSAR decision support can be made by comparing POS values. The TS-PSO algorithm provides a new theoretical basis for the field of MSAR mission area planning, and the heuristic algorithm represented by this algorithm can also be applied in this field and other related fields.

ACKNOWLEDGMENT

The authors are grateful to Mr. Bin Wang, Mr. Hao Yang, and Mr. PengXiang Yin in Donghai No. 2 Flying Service of Ministry Of Transport, Xiamen, China, for providing valuable experience of helicopter MSAR mission. They also thank the anonymous reviewers for their critical and constructive review of the manuscript

REFERENCES

[1] J. R. Frost, *The Theory of Search: A Simplified Explanation*. Richmond, VA, USA: Soza & Company, U.S. Coast Guard Office of Search and Rescue, 1996.
[2] J. R. Frost and L. D. Stone, "Review of search theory: Advances and applications to search and rescue decision support," U.S. Coast Guard Res. Develop. Center, Groton, MA, USA, Tech. Rep. CG-D-15-01, Sep. 2001.
[3] L. D. Stone, *Theory of Optimal Search*. New York, NY, USA: Academic, 1975.
[4] M. L. Spaulding and E. Howlett, "Application of SARMAP to estimate probable search area for objects lost at sea," *Oceanogr. Lit. Rev.*, vol. 5, no. 44, p. 523, 1997.
[5] T. M. Kratzke, L. D. Stone, and J. R. Frost, "Search and rescue optimal planning system," in *Proc. 13th Int. Conf. Inf. Fusion*, Jul. 2010, pp. 1–8.
[6] H. R. Richardson and J. H. Discenza, "The united states coast guard computer-assisted search planning system (CASP)," *Nav. Res. Logistics Quart.*, vol. 27, no. 4, pp. 659–680, Dec. 1980.
[7] F. B. Xiao, "Research on the Key Technologies of Maritime Search and Rescue Decision Support System," Ph.D. dissertation, Key Lab. Mar. Simul. Control, Dalian Maritime Univ., Dalian, China, Aug. 2011.
[8] D. A. Otote, B. Li, B. Ai, S. Gao, J. Xu, X. Chen, and G. Lv, "A decision-making algorithm for maritime search and rescue plan," *Sustainability*, vol. 11, no. 7, p. 2084, Apr. 2019.
[9] B. Ai, B. Li, S. Gao, J. Xu, and H. Shang, "An intelligent decision algorithm for the generation of maritime search and rescue emergency response plans," *IEEE Access*, vol. 7, pp. 155835–155850, 2019, doi: 10.1109/ACCESS.2019.2949366.
[10] W. Yue, Y. Xi, and X. Guan, "A new searching approach using improved multi-ant colony scheme for multi-UAVs in unknown environments," *IEEE Access*, vol. 7, pp. 161094–161102, Oct. 2019, doi: 10.1109/ACCESS.2019.2949249.
[11] A. A. Nagra, F. Han, Q.-H. Ling, and S. Mehta, "An improved hybrid method combining gravitational search algorithm with dynamic multi swarm particle swarm optimization," *IEEE Access*, vol. 7, pp. 50388–50399, 2019, doi: 10.1109/ACCESS.2019.2903137.
[12] K. J. Rafferty and E. W. McGookin, "An autonomous air-sea rescue system using particle swarm optimization," in *Proc. Int. Conf. Connected Vehicles Expo (ICCVE)*, Dec. 2013, pp. 459–464, doi: 10.1109/ICCVE.2013.6799836.
[13] J. Lv, M. Liu, H. Zhao, B. Li, and S. Sun, "Maritime static target search based on particle swarm algorithm," in *Proc. SAI Intell. Syst. Conf.*, Aug. 2016, pp. 917–927.
[14] J. Liu, H. Ma, X. Ren, T. Shi, P. Li, and X. Ma, "The continuous-discrete PSO algorithm for shape formation problem of multiple agents in two and three dimensional space," *Appl. Soft Comput.*, vol. 67, pp. 409–433, Jun. 2018, doi: 10.1016/j.asoc.2018.02.015.
[15] X. Ye, B. Chen, P. Li, L. Jing, and G. Zeng, "A simulation-based multi-agent particle swarm optimization approach for supporting dynamic decision making in marine oil spill responses," *Ocean Coastal Manage.*, vol. 172, pp. 128–136, Apr. 2019, doi: 10.1016/j.ocecoaman.2019.02.003.
[16] J. Sánchez-García, D. G. Reina, and S. L. Toral, "A distributed PSO-based exploration algorithm for a UAV network assisting a disaster scenario," *Future Gener. Comput. Syst.*, vol. 90, pp. 129–148, Jan. 2019, doi: 10.1016/j.future.2018.07.048.
[17] Y. Wang, P. Bai, X. Liang, W. Wang, J. Zhang, and Q. Fu, "Reconnaissance mission conducted by UAV swarms based on distributed PSO path planning algorithms," *IEEE Access*, vol. 7, pp. 105086–105099, 2019, doi: 10.1109/ACCESS.2019.2932008.
[18] *International Aeronautical and Maritime Search and Rescue Manual*, IMO/ICAO, Montreal, QC, Canada, 2013.
[19] Ø. Breivik and A. A. Allen, "An operational search and rescue model for the Norwegian sea and the north sea," *J. Mar. Syst.*, vol. 69, nos. 1–2, pp. 99–113, Jan. 2008.
[20] Z. Ni, Z. Qiu, and T. C. Su, "On predicting boat drift for search and rescue," *Ocean Eng.*, vol. 37, no. 13, pp. 1169–1179, Sep. 2010.
[21] Ø. Breivik, A. A. Allen, C. Maisondieu, and J. C. Roth, "Wind-induced drift of objects at sea: The leeway field method," *Appl. Ocean Res.*, vol. 33, no. 2, pp. 100–109, Apr. 2011.
[22] S. J. Meng, H. Wang, W. Lu, Z. Y. Wang, and Y. Li, "Drift trajectory model of the unpowered vessel on the sea and its application in the drift simulation of the SANCHI oil tanker," *Oceanologia Et Limnologia Sinica*, vol. 49, no. 2, pp. 242–250, Mar. 2018.
[23] X. J. Liu and K. Zhang, "The study of marine drift model based on Monte Carlo method," *China Water Transp.*, vol. 17, no. 9, pp. 32–34 and 36, Sep. 2017.
[24] S.-Z. Wang, H.-B. Nie, and C.-J. Shi, "A drifting trajectory prediction model based on object shape and stochastic motion features," *J. Hydrodyn.*, vol. 26, no. 6, pp. 951–959, Dec. 2014.
[25] B. A. Brushett, A. A. Allen, B. A. King, and C. J. Lemckert, "Application of leeway drift data to predict the drift of panga skiffs: Case study of maritime search and rescue in the tropical pacific," *Appl. Ocean Res.*, vol. 67, pp. 109–124, Sep. 2017.
[26] A. W. Heemink, "Stochastic modelling of dispersion in shallow water," *Stochastic Hydrol. Hydraul.*, vol. 4, no. 2, pp. 161–174, Jun. 1990.
[27] K. N. Dimou and E. E. Adams, "A random-walk, particle tracking model for well-mixed estuaries and coastal waters," *Estuarine, Coastal Shelf Sci.*, vol. 37, no. 1, pp. 99–110, Jul. 1993.

[28] D. Brickman and P. C. Smith, "Lagrangian stochastic modeling in coastal oceanography," *J. Atmos. Ocean. Technol.*, vol. 19, no. 1, pp. 83–99, Jan. 2002.
[29] D. S. Wang, X. D. Liu, and H. D. Zhuang, "An Improved maritime search and rescue area prediction method and system," U.S. Patent CN 105 653 826 A, Oct. 3, 2016.
[30] *National Maritime Search and Rescue Support System*. Accessed: Jul. 13, 2018. [Online]. Available: http://marinesar.cn/index.html
[31] H. Liu, Z. K. Chen, Y. L. Tian, B. Wang, H. Yang, and G. H. Wu, "Evaluation method for helicopter maritime search and rescue response plan with uncertainty," *Chin. J. Aeronaut.*, to be published.
[32] B. O. Koopman, "The theory of Search. II. Target detection," *Oper. Res.*, vol. 4, no. 5, pp. 503–531, Oct. 1956.
[33] J. de Guenin, "Optimum distribution of effort: An extension of the koopman basic theory," *Oper. Res.*, vol. 9, no. 1, pp. 1–7, Feb. 1961.
[34] L. D. Stone, "Search and screening: General principles with historical applications (B. O. Koopman)," *SIAM Rev.*, vol. 23, no. 4, pp. 533–539, Oct. 1981.
[35] G. T. Toussaint, "Solving geometric problems with the rotating calipers," in *Proc. IEEE Melecon*, vol. 83, May 1983, p. A10.
[36] N. Jia, Y. You, Y. Lu, Y. Guo, and K. Yang, "Research on the search and rescue System-of-Systems capability evaluation index system construction method based on weighted supernetwork," *IEEE Access*, vol. 7, pp. 97401–97425, Jul. 2019, doi: 10.1109/ACCESS.2019.2929235.
[37] H. Lee, N. Aydin, Y. Choi, S. Lekhavat, and Z. Irani, "A decision support system for vessel speed decision in maritime logistics using weather archive big data," *Comput. Oper. Res.*, vol. 98, pp. 330–342, Oct. 2018.
[38] C. H. Yang, C. J. Hsiao, and L. Y. Chuang, "Linearly decreasing weight particle swarm optimization with accelerated strategy for data clustering," *IAENG Int. J. Comput. Sci.*, vol. 37, no. 3, p. 1, Aug. 2010.
[39] D. C. Cooper, J. R. Frost, and R. Q. Robe, "Compatibility of land SAR procedures with search theory," Potomac Manage. Group, Alexandria, VA, USA, Tech. Rep. 0704-0188, Jan. 2003.

ZIKUN CHEN was born in Tianjin, China, in 1992. He received the B.E. and M.E. degrees in flight vehicle design from the Harbin Institute of Technology, in 2014 and 2016, respectively. He is currently pursuing the Ph.D. degree in aircraft design with the School of Aeronautic Science and Engineering, Beihang University. His main research areas are aircraft conceptual design, decision support for helicopter operation, and system of systems simulation. He is a member of the Chinese Society of Aeronautics and Astronautics (CSAA).

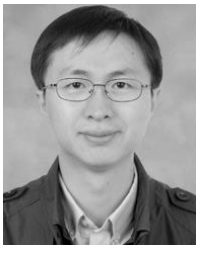

HU LIU received the B.S. and Ph.D. degrees in aircraft design from Beihang University (formerly Beijing University of Aeronautics and Astronautics), Beijing, China, in 2000 and 2004, respectively. He is currently the Head of the Aircraft Department and a Professor with Beihang University. He is a member of the American Institute of Aeronautics and Astronautics (AIAA) and the Chinese Society of Aeronautics and Astronautics (CSAA). He is a Main Instructor of Aircraft Conceptual Design, which is a national quality curriculum. His main research areas are aircraft conceptual design and training support technologies.

YONGLIANG TIAN received the B.S. degree in aircraft design and engineering and the Ph.D. degree in aircraft design from Beihang University, Beijing, in 2009 and 2015, respectively.

From 2013 to 2014, he studied with the School of Aeronautics and Aerospace Engineering, Purdue University, USA, as a Visiting Student. From 2016 to 2018, he was with the Shanghai Aircraft Design and Research Institute, Commercial Aircraft Corporation of China Ltd. Since 2018, he has conducted postdoctoral research in mechanics with Beihang University. He has published more than 15 articles in academic publications. His main research areas are aircraft conceptual design and system engineering, including conceptual software systems, virtual simulation technology, intelligent design technology, and so on. He is a member of the Chinese Society of Aeronautics and Astronautics (CSAA). He received the FRONTRUNNER 5000–Top Articles in Outstanding Science and Technology Journal of China awarded by the China Institute of Science and Technology Information, in 2013.

RUI WANG was born in 1997. He received the bachelor's degree in engineering mechanics from Beihang University, Beijing, China, in 2019, where he is currently pursuing the master's degree in aircraft design and engineering with the School of Aeronautic Science and Engineering. His research interests include system simulation and operational effectiveness evaluation.

PEISEN XIONG was born in Chengdu, Sichuan, China, in 1993. He received the B.E. degree in aircraft design from Beihang University, in 2015, where he is currently pursuing the Ph.D. degree in aircraft design with the School of Aeronautic Science and Engineering. His current research interests include operational research, system of systems, and agent-based simulation.

GUANGHUI WU was born in 1960. He received the B. S. degree in aircraft design from the Nanjing University of Aeronautics and Astronautics, Nanjing, China, in 1982, and the Ph.D. degree from Beihang University, in 2009. He was elected as an Academician of the Chinese Academy of Engineering, in 2017. He has been the Chief Designer of ARJ21. He is currently a member of the Standing Committee of the Party Committee, the Vice President, and the Chief Designer of the C919 Program at Commercial Aircraft Corporation of China, Ltd. (COMAC).